The Origin of Green Emission of ZnO Microcrystallites: Surface-Dependent Light Emission Studied by Cathodoluminescence

Xi Zhou, Qin Kuang, Zhi-Yuan Jiang, Zhao-Xiong Xie,* Tao Xu, Rong-Bin Huang, and Lan-Sun Zheng

State Key Laboratory for Physical Chemistry of Solid Surfaces & Department of Chemistry, College of Chemistry and Chemical Engineering, Xiamen University, Xiamen 361005, China

Received: March 9, 2007; In Final Form: June 7, 2007

Green emission of ZnO microcrystallites has been studied in detail by directly investigating the luminescence from the different crystal surfaces of ZnO microcrystallites by means of room temperature cathodoluminescence (CL). The relative strength of the green emission was found to be strongly dependent on the crystal surfaces. By discussing the atom structures of different crystal surfaces, it is concluded that the green emission mostly comes from the defects on/near the surfaces.

Introduction

Anisotropy is a basic property of single crystals. Various facets or surfaces on a crystal may have different structures and atomic densities, which exhibit different physical and chemical properties. For small particles, especially, in micro-/nanometric scale, the surface area becomes very large and therefore may dominate some of their physical and chemical properties. In recent years, numerous studies have been focused on the nanomaterials because materials in nanometric scale may exhibit some special properties in contrast to their bulk phases. Although it is well-known that the surfaces are very important in nanomaterials and many studies concerning surface effects on the chemical properties such as catalytic activities have been studied,[1−4] less attention has been paid to the surface effects on the physical properties of small crystallites.

Zinc oxide (ZnO) has attracted considerable attention for promising applications in optoelectronic devices due to its wide band gap (3.37 eV) and large exciton binding energy (60 meV). Better understanding of the optical process in ZnO crystals certainly benefits the practical applications of ZnO. For this reason, the optical properties of various forms of ZnO, including ZnO nanostructures, have been extensively studied by photoluminescence (PL) spectroscopy at both room temperature and variable-temperature conditions.[5] The experiments so far show that room temperature PL spectra of ZnO typically consist of a UV emission and sometimes one or more visible bands due to defects and/or impurities.[5] Among the visible bands, green emission has been commonly thought to be the defect emission in ZnO crystals. Several different hypotheses have been proposed to explain the origin of the green emission, such as singly ionized oxygen vacancies,[6−10] antisite oxygen,[11] oxygen vacancies and zinc interstitials,[12] and impurities.[13,14] Recently, Djurišić et al. proposed that the green emission of ZnO nanostructures originated from surface defects based on that green emissions were suppressed by coating ZnO nanostrustures with surfactants.[15] Similar phenomenon has also been observed with a surface shell of $Zn(OH)_2$ enclosing ZnO nanostructures.[16] Very recently, we found that the green emission can be induced by constructing the epitaxial hetrostructural interface between the SnO_2 and ZnO nanostructures.[17] These results indicate that the surfaces and interfaces play a key role in the green emissions of the nanocrystals. However, it still lacks direct and detailed evidence for the origin of the green emissions. The identification of the exact origin of this green emission therefore remains a great challenge. In this study, the room temperature cathodoluminescence (CL) has been applied to directly detect the luminescence from different crystal surfaces of ZnO microcrystallites. Surface-dependent green emissions have been observed, which demonstrate that the green emission mostly comes from the defects on/near the surface of the ZnO microcrystallites.

Experimental Section

The optical measurements were performed on ZnO micropyramids and ZnO nanorods synthesized by the thermal decomposition of $Zn(Ac)_2$ in different solvents as reported in our previous paper.[18] The morphology of the nanostructures was examined by scanning electron microscopy (SEM), using a LEO 1530 field emission SEM. Photoluminescence (PL) spectra were obtained at room temperature with a Hitachi luminescence spectrometer (F-4500), using a Xenon discharge lamp as the excitation light source and an excitation wavelength of 325 nm. The room temperature cathodoluminescence (CL) measurements were carried out in situ in the LEO1530 SEM integrated with a Gatan MonoCL cathodoluminescence system. An accelerate voltage of 20 kV was used. Each CL measurement was taken in a previously unexposed area to avoid the possible influence of electron irradiation.

Results and Discussion

The investigation of the luminescence properties of ZnO nanocrystals was started with the acquisition of room temperature PL spectra of ZnO micropyramids and ZnO nanorods, as shown in Figure 1. As has been reported in our previous paper, the micropyramid with the base size of around 1 μm (Figure 1A) is enclosed by six $\{10\bar{1}1\}$ side surfaces and one $(000\bar{1})$ base plane, and the nanorod (Figure 1B) with diameters of about 100 nm is exposed with six $\{10\bar{1}0\}$ planes; and all the exposed surfaces are very smooth.[18] In the corresponding PL spectra (Figure 1C), the typical two emission peaks (a narrow peak at

* Address correspondence to this author. E-mail: zxxie@xmu.edu.cn.

10.1021/jp071928h CCC: $37.00
Published on Web 07/21/2007

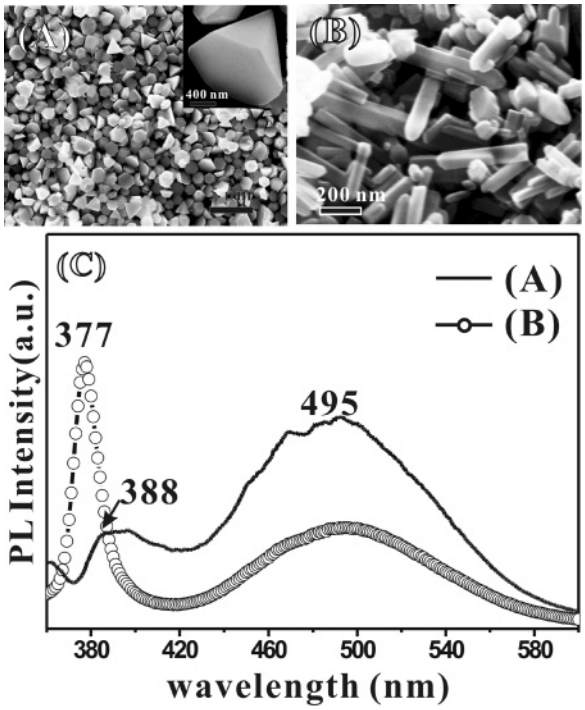

Figure 1. (A) SEM image of the ZnO micropyramid, (B) SEM image of the ZnO nanorod, and (C) room temperature PL spectra of the ZnO micropyramid (A), and ZnO nanorod (B).

about 377−387 nm and a broad peak at 495 nm) were observed in both of these ZnO nanostructures, which were assigned to the UV emission and green emission, respectively. Although two kinds of samples show similar UV and green emissions, the green-to-UV emission ratios are very different between the two samples. For the micropyramids, the green emission is strong and the UV emission becomes relatively weak. On the contrary, the nanorod shows a weak green emission in contrast to the UV emission.

Further insight into the origin of the light emission was carried out by directly studying the emission from different crystal planes on these two ZnO nanostructures with the CL technique. Figure 2 shows three typical CL spectra taken from three different crystal faces: the pyramidal $\{10\bar{1}1\}$ planes, the basal $(000\bar{1})$ plane from the micropyramid, and the prismatic $\{10\bar{1}0\}$ planes from the nanorod. It should be noted that these three types of crystal planes chosen for CL measurement are typical low-index crystal surfaces for the wurzite ZnO nanostructures, although $\{10\bar{1}1\}$ is scarcely exposed. From the CL spectra, it can be observed that the relative strength of the green emission peak is dependent on the crystal planes. The spectrum recorded from the $\{10\bar{1}1\}$ plane exhibits a dominant green luminescence in contrast to the UV emission, as shown in Figure 2A. For the case of the $(000\bar{1})$ plane, the intensity of UV emission exceeds that of green emission as shown in Figure 2B. That is to say, for the same crystallite, the intensities of green emissions are surface- or direction-dependent. In the present case, the penetration depth of the injected electrons could be tens of nanometers with the accelerating voltage of 20 kV, which would result in green emissions from both the bulk and surfaces. As the green emission intensities should be the same for those originating from the bulk, we conclude that the differences of the green emissions can be attributed to the difference of surfaces. To explore the green emission from the prismatic $\{10\bar{1}0\}$ planes, the ZnO nanorods were chosen instead. The results show that the green emission is very weak and the UV emission becomes relatively strong as shown in Figure 2C. The green-to-UV emission ratio is the lowest among these three planes. As a result, the relative intensity of green emission in contrast to the UV emission from the $\{10\bar{1}1\}$ plane is the highest, while that from the $(000\bar{1})$ plane is medium, and that from the $\{10\bar{1}0\}$ plane is the lowest one.

The green luminescence behaviors of the three different planes show the surface-dependent properties, indicating that the green luminescence would be related to the atomic structure at the surface of the crystal. As the defects are responsible for the green emission, the possible defects on/near the surfaces should be clarified for the explanations of surface-dependent green emission intensity. On a crystal surface, the periodicity of the crystal breaks, which results in the appearance of dangling bonds on surface atoms. The real surfaces usually reconstruct or adsorb additional atoms/molecules to eliminate the dangling bonds of the surface atoms. In fact, in comparison with the bulk lattice, the surface atoms look like a kind of defect. The anisotropic property of the crystal determines that different kinds of crystal surfaces have different defects. Figure 3 shows the schematic model of the atomic structures on $\{10\bar{1}0\}$, $(000\bar{1})$, and $\{10\bar{1}1\}$ crystal surfaces of ZnO, respectively. It should be

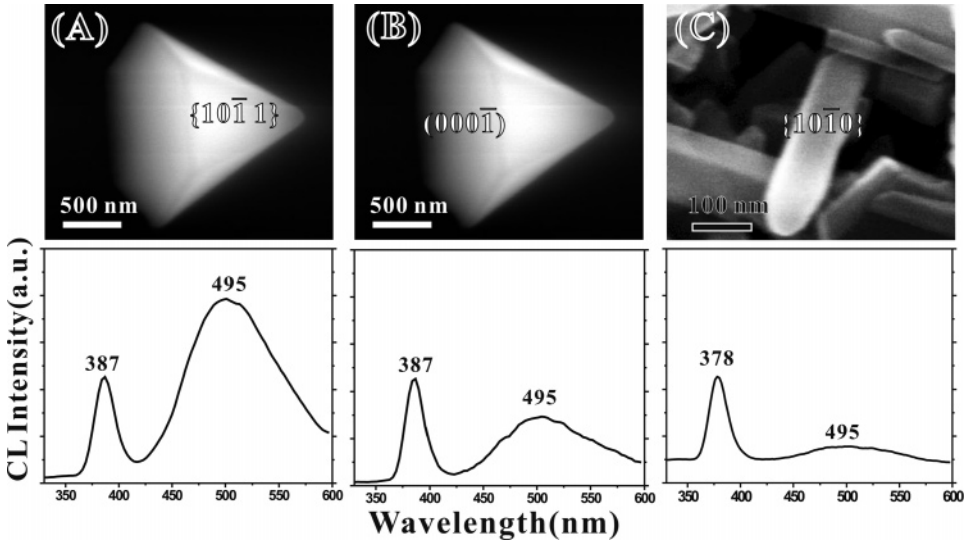

Figure 2. Room temperature CL spectra recorded from three different crystal faces: (A) the pyramidal $\{10\bar{1}1\}$ planes, (B) the basal $(000\bar{1})$ plane, and (C) the prismatic $\{10\bar{1}0\}$ planes as labeled in the SEM images.

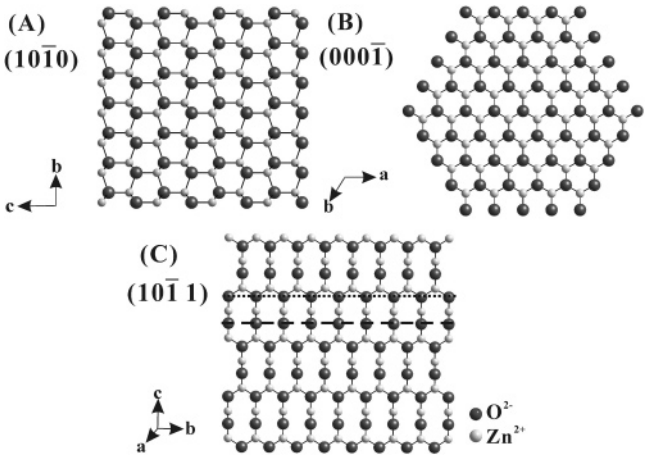

Figure 3. Schematic models of the atomic structures on different crystal surfaces of ZnO: (A) {10$\bar{1}$0}, (B) (000$\bar{1}$), and (C) {10$\bar{1}$1}

noted that the oxygen-terminated (000$\bar{1}$) and {10$\bar{1}$1} planes are adopted in the corresponding models, as anions have a larger atomic radius and are easily polarized to stabilize the surfaces. For the wurtzite ZnO crystal, the [0001] and [10$\bar{1}$1] directions are the polar direction, while the [10$\bar{1}$0] direction is nonpolar. The corresponding (000$\bar{1}$) and {10$\bar{1}$1} surfaces are therefore polar surfaces, and the {10$\bar{1}$0} surface is nonpolar. The nonpolar {10$\bar{1}$0} surfaces are electrically neutral. They have relatively low surface energy and thus very low defect should present on the surface. As defects are known to be responsible for the green emissions, the {10$\bar{1}$0} surfaces have very weak green emissions. However, on the polar (000$\bar{1}$) surface as shown in Figure 3B, an oxygen atom bonds to three of the underneath Zn atoms, while it bonds to four Zn atoms in the ZnO bulk. Therefore, every surface O atom has $^2/_3$ extra charges (every O atom has two negative charges). The surface needs reconstruction to form a stable surface. Very possibly, the oxygen vacancies form on/near the surface to eliminate the surplus charges. The oxygen vacancies have been thought to be the source of the green emission, and thus green emission appears on the (000$\bar{1}$) plane. For the {10$\bar{1}$1} surface as shown in Figure 3C, half of the O atoms connect to three Zn atoms (marked by dot line), and another half of the O atoms only coordinate to two Zn atoms (marked by dash line). The average surplus charge of one surface O atom is then $^5/_6$, which is much larger than that of the (000$\bar{1}$) surface. The polarity of the {10$\bar{1}$1} surface is then larger than that of the (000$\bar{1}$) surface. Therefore the surface energy of the {10$\bar{1}$1} surface is higher, and usually the {10$\bar{1}$1} surfaces do not appear as the bare surfaces during the crystal growth. Being similar to the (000$\bar{1}$) surface, the {10$\bar{1}$1} surfaces need to eliminate the surplus charges to form the stable surface when they are exposed. As the surplus charges on the {10$\bar{1}$1} surfaces are larger than that on the (000$\bar{1}$) surfaces, there should be many more oxygen vacancies formed on/near the surface. Therefore more intense green emissions are observed on the {10$\bar{1}$1} surfaces than on the (000$\bar{1}$) surfaces.

It is well-known that the UV emission corresponds to the near band-edge emission. By comparing the UV emissions from the micropyramids with those from the nanorods, it can be found that the UV peak from micropyramids shows a little red shift as shown in the CL spetra (Figure 2). The micropyramid, with base size around 1 μm, shows the same UV emissions from different crystal surfaces (peak center at 387 nm), while for the nanorod with a diameter about 100 nm, the UV emission is located at 378 nm. It seems the UV emissions have a red shift with the increase of the particle size. However, the shift of the UV peaks is not due to the quantum confinement effect, as the particle size of the ZnO crystals is far larger than the Bohr radius of ZnO (2.34 nm).[5,19] The differences in these UV emissions could be due to different concentrations of native defects in the two ZnO crystallites.

By the combination of the PL and the CL results, the different green-to-UV emission ratio between the ZnO micropyramid and the ZnO nanorod can be well explained. Since the micropyramid is enclosed by six pyramidal {10$\bar{1}$1} planes with high defect levels and only one base (000$\bar{1}$) plane with a low defect level, the micropyramids exhibit a relatively high intensity of green emission. As for the nanorods, they are exposed with six prismatic {10$\bar{1}$0} planes that have low defect levels, and therefore a weak green emission from the nanorods is observed.

In conclusion, the surface-dependent green luminescences of ZnO microcrystallites were observed by the CL technique. It was demonstrated that the green emission mostly originated from the defects on/near the surface. Apart from providing direct evidence for the origin of green emission, it is also anticipated that optical properties of the ZnO micro-/nanocrystallites are tunable through the control of the crystal surfaces. The present study will certainly give a great impetus to the applications of the surface architecture-controlled ZnO micro-/nanomaterials in optoelectronic devices.

Acknowledgment. This work was supported by the National Natural Science Foundation of China (Grant Nos. 20673085, 20473069, and 20671078), the Key Scientific Project of Fujian Province of China (Grant No. 2005HZ01-3), NCET from the Ministry of Education of China, and the Fok Ying-Tung Educational Foundation.

References and Notes

(1) Over, H.; Kim, Y. D.; Seitsonen, A. P.; Wendt, S.; Lundgren, E.; Schmid, M.; Varga, P.; Morgante, A.; Ertl, G. *Science* **2000**, *287*, 1474.

(2) Roeffaers, M. B. J.; Sels, B. F.; Uji-i, H.; De Schryver, F. C.; Jacobs, P. A.; De Vos, D. E.; Hofkens, J. *Nature* **2006**, *439*, 572.

(3) Somorjai, G. A.; Borodko, Y. G. *Catal. Lett.* **2001**, *76*, 1.

(4) Rosei, F. *J. Phys.*: *Condens. Matter* **2004**, *16*, S1373.

(5) Djurišić, A. B.; Leung, Y. H. *Small* **2006**, *2*, 944.

(6) Meng, X. Q.; Shen, D. Z.; Zhang, J. Y.; Zhao, D. X.; Lu, Y. M.; Dong, L.; Zhang, Z. Z.; Liu, Y. C.; Fan, X. W. *Solid State Commun.* **2005**, *135*, 179.

(7) Chen, Y. Q.; Jiang, J.; He, Z. Y.; Su, Y.; Cai, D.; Chen, L. *Mater. Lett.* **2005**, *59*, 3280.

(8) Wang, R. C.; Liu, C. P.; Huang, J. L.; Chen, S. J. *Appl. Phys. Lett.* **2005**, *87*, 053103.

(9) Ng, H. T.; Chen, B.; Li, J.; Han, J.; Meyyappan, M.; Wu, J.; Li, S. X.; Haller, E. E. *Appl. Phys. Lett.* **2003**, *82*, 2023.

(10) Chen, Z.; Wu, N. Q.; Shan, Z. W.; Zhao, M. H.; Li, S. X.; Jiang, C. B.; Chyu, M. K.; Mao, S. X. *Scr. Mater.* **2005**, *52*, 63.

(11) Yang, Q.; Tang, K.; Zuo, J.; Qian, Y. *Appl. Phys. A* **2004**, *79*, 1847.

(12) Liu, X.; Wu, X. H.; Cao, H.; Chang, R. P. H. *J. Appl. Phys.* **2004**, *95*, 3141.

(13) Garces, N. Y.; Wang, L.; Bai, L.; Giles, N. C.; Halliburton, L. E.; Cantwell, G. *Appl. Phys. Lett.* **2002**, *81*, 622.

(14) Sekiguchi, T.; Miyashita, S.; Obara, K.; Shishido, T.; Sakagami, N. *J. Cryst. Growth* **2000**, *214*, 72.

(15) Djurišić, A. B.; Choy, W. C. H.; Roy, V. A. L.; Leung, Y. H.; Kwong, C. Y.; Cheah, K. W.; Rao, T. K. G.; Chan, W. K.; Lui, H. F.; Surya, C. *Adv. Funct. Mater.* **2004**, *14*, 856.

(16) Zhou, H.; Alves, H.; Hofmann, D. M.; Kriegseis, W.; Meyer, B. K.; Kaczmarczyk, G.; Hoffmann, A. *Appl. Phys. Lett.* **2002**, *80*, 210.

(17) Kuang, Q.; Jiang, Z. Y.; Xie, Z. X.; Lin, S. C.; Lin, Z. W.; Xie, S. Y.; Huang, R. B.; Zheng, L. S. *J. Am. Chem. Soc.* **2005**, *127*, 11777.

(18) Zhou, X.; Xie, Z. X.; Jiang, Z. Y.; Kuang, Q.; Zhang, S. H.; Xu, T.; Huang, R. B.; Zheng, L. S. *Chem. Commun.* **2005**, 5572.

(19) Gu, Y.; Kuskovsky, I. L.; Yin, M.; O'Brien, S.; Neumark, G. F. *Appl. Phys. Lett.* **2004**, *85*, 3833.